RESEARCH ARTICLE

Figures and figure supplements

The mTOR pathway genes *MTOR*, *Rheb*, *Depdc5*, *Pten*, and *Tsc1* have convergent and divergent impacts on cortical neuron development and function

Lena H Nguyen *et al*.

Figure 1. Expression of *Rheb*^{Y35L}, *MTOR*^{S2215Y}, *Depdc5*^{KO}, *Pten*^{KO}, and *Tsc1*^{KO} leads to varying magnitudes of neuronal enlargement and mispositioning in the cortex. (**a**) Diagram of the PI3K-mTORC1 pathway. Activation of mTOR complex 1 (mTORC1) signaling is controlled by positive (blue) and negative (purple) regulators within the pathway. (**b**) Diagram of overall experimental timeline and approach. in utero electroporation (IUE) was performed at E15.5. A cohort of animals was used for patch clamp recording at P26-51 and another cohort was used for histology at P28-43. (**c**) Representative images of tdTomato+ cells (red) and p-S6 staining (green) in mouse medial prefrontal cortex (mPFC) at P28-43. (**d**) Quantification of p-S6 staining intensity (normalized to the mean control) in tdTomato+ neurons. (**e**) Quantification of tdTomato+ neuron soma size. (**f**) Representative images of tdTomato+ neuron (red) placement and distribution in coronal mPFC sections. Red square on the diagram denotes the imaged area for all groups. CC, corpus callosum. (**g**) Quantification of tdTomato+ neuron placement in layer 2/3. Left diagram depicts the approach for analysis: the total number of tdTomato+ neurons within layer 2/3 (white square) was counted and expressed as a % of total neurons in the imaged area. Right bar graphs show the quantification.

Figure 1 continued on next page

Figure 1 continued

(**h**) Quantification of tdTomato+ neuron distribution across cortical layers. Left diagram depicts the approach for analysis: the imaged area was divided into 10 equal-sized bins across the cortex, spanning the corpus callosum to the pial surface (white grids); the total number of tdTomato+ neurons within each bin was counted and expressed as a % of total neurons in the imaged area. Right bar graphs show the quantification. For graphs (**d, e**): n=4–8 mice per group, with 6–15 cells analyzed per animal. For graphs (**g, h**): n=3–7 mice per group, with 1 brain section analyzed per animal. Statistical comparisons were performed using (**d, e**) nested one-way ANOVA (fitted to a mixed-effects model) to account for correlated data within individual animals, (**g**) one-way ANOVA, or (**h**) two-way repeated measures ANOVA. Post-hoc analyses were performed using Holm-Šídák multiple comparison test. *p<0.05, **p<0.01, ***p<0.001, ****p<0.0001. All data are reported as the mean of all neurons or brain sections in each group ± SEM.

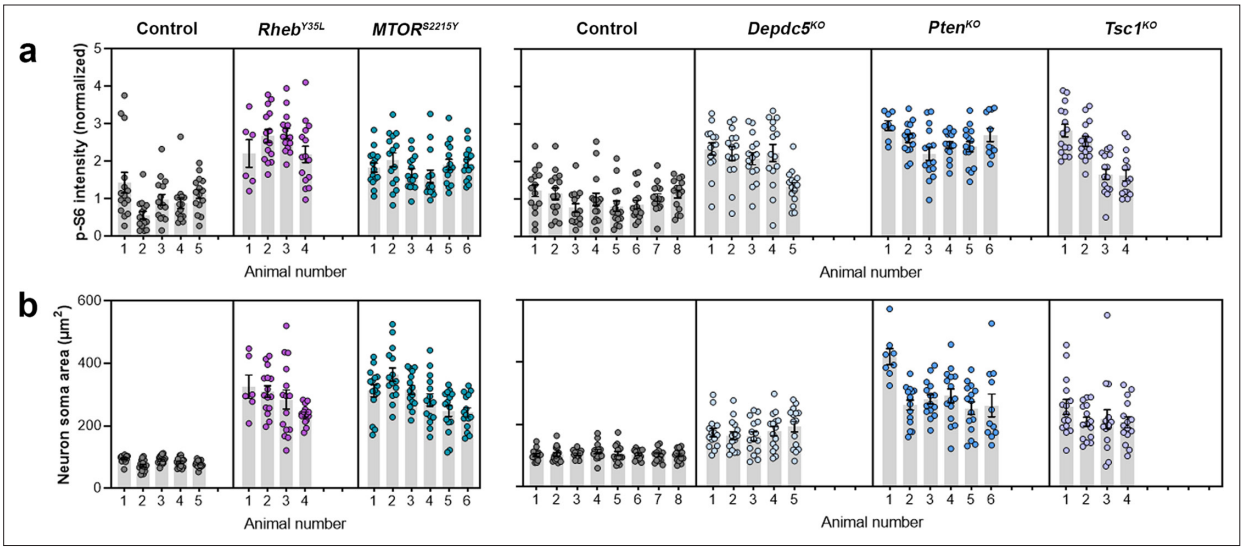

Figure 1—figure supplement 1. Distribution of p-S6 staining intensity and neuron soma size among individual animals at P28-43. (**a**) Distribution of p-S6 staining intensity among individual animals. (**b**) Distribution of neuron soma size among individual animals.

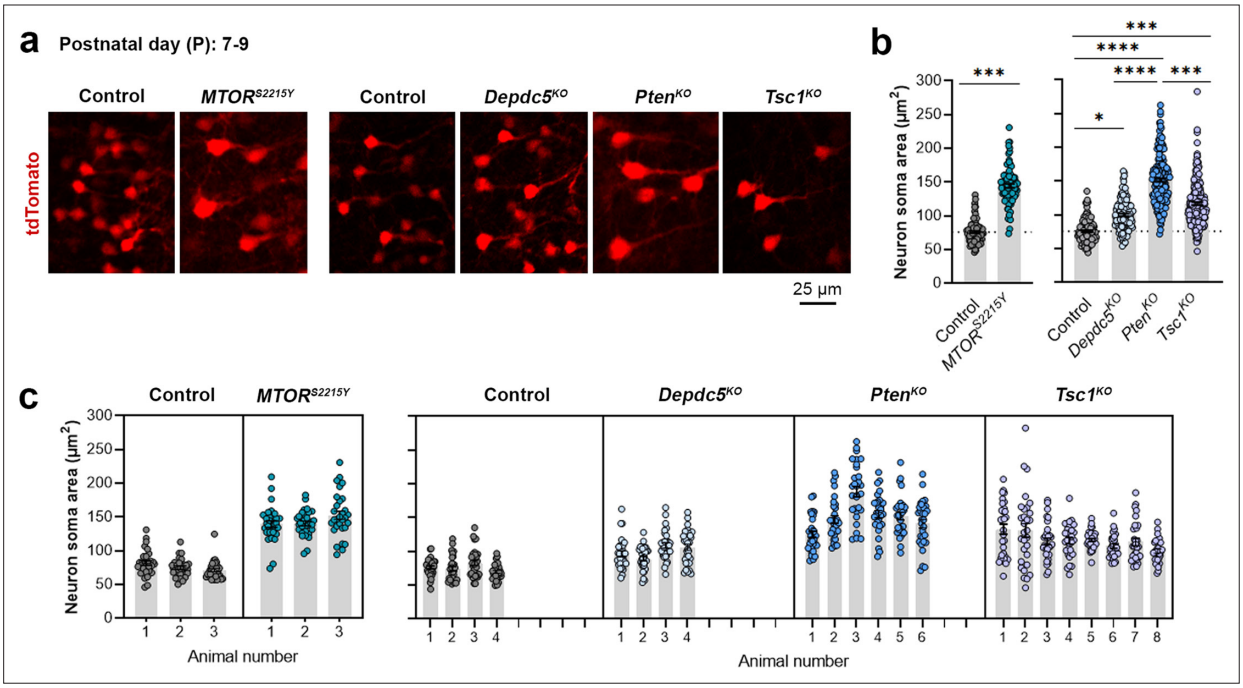

Figure 1—figure supplement 2. Neuron soma sizes at P7-9. (**a**) Representative images of tdTomato+ cells (red) in mouse medial prefrontal cortex (mPFC) at P7-9. (**b**) Quantification of tdTomato+ neuron soma size. (**c**) Graph showing the distribution of neuron soma size among individual animals in each group. n=3–8 mice per group, with 30 cells analyzed per animal. Statistical comparisons were performed using a nested t-test (control vs. *MTOR*^{S2215Y}) or nested one-way ANOVA (control vs. *Depdc5*^{KO} vs. *Pten*^{KO}, vs. *Tsc1*^{KO}) (fitted to a mixed-effects model) to account for correlated data within individual animals. Post-hoc analyses were performed using Holm-Šídák multiple comparison test. *p<0.05, ***p<0.001, ****p<0.0001. Data are reported as the mean of all neurons in each group ± SEM.

Figure 2. Expression of *Rheb*^{Y35L}, *MTOR*^{S2215Y}, *Depdc5*^{KO}, *Pten*^{KO}, and *Tsc1*^{KO} universally leads to decreased depolarization-induced excitability, but only *Rheb*^{Y35L}, *MTOR*^{S2215Y}, and *Tsc1*^{KO} expression leads to depolarized resting membrane potentials (RMPs). (**a**) Diagram of experimental approach for whole-cell patch clamp recording. Recordings were performed in layer 2/3 pyramidal neurons in acute coronal slices from P26-51 mice, expressing either control, *Rheb*^{Y35L}, *MTOR*^{S2215Y}, *Depdc5*^{KO}, *Pten*^{KO}, or *Tsc1*^{KO} plasmids. (**b–d**) Graphs of membrane capacitance, resting membrane conductance, and RMP. (**e**) Representative traces of the action potential (AP) firing response to a 300 pA depolarizing current injection. (**f**) Input-output curves show the mean number of APs fired in response to 500 ms-long depolarizing current steps from 0 to 400 pA. Arrows point to initial spike doublets. (**g–k**) Graphs of rheobase, first ISI, AP threshold, AP peak amplitude, and AP half-width. For all graphs: n=5–10 mice per group, with 16–50 cells analyzed per animal.

Figure 2 continued on next page

Figure 2 continued

Statistical comparisons were performed using (**b–d, g–k**) nested one-way ANOVA (fitted to a mixed-effects model) to account for correlated data within individual animals or (**f**) mixed-effects ANOVA accounting for repeated measures. Post-hoc analyses were performed using Holm-Šídák multiple comparison test. *p<0.05, **p<0.01, ***p<0.001, ****p<0.0001, for the input-output curves in (**f**): *p<0.05 (vs. control), #<0.05 (vs. *Depdc5*^{KO}), ₮p<0.05 (vs. *Tsc1*^{KO}). All data are reported as the mean of all neurons in each group ± SEM.

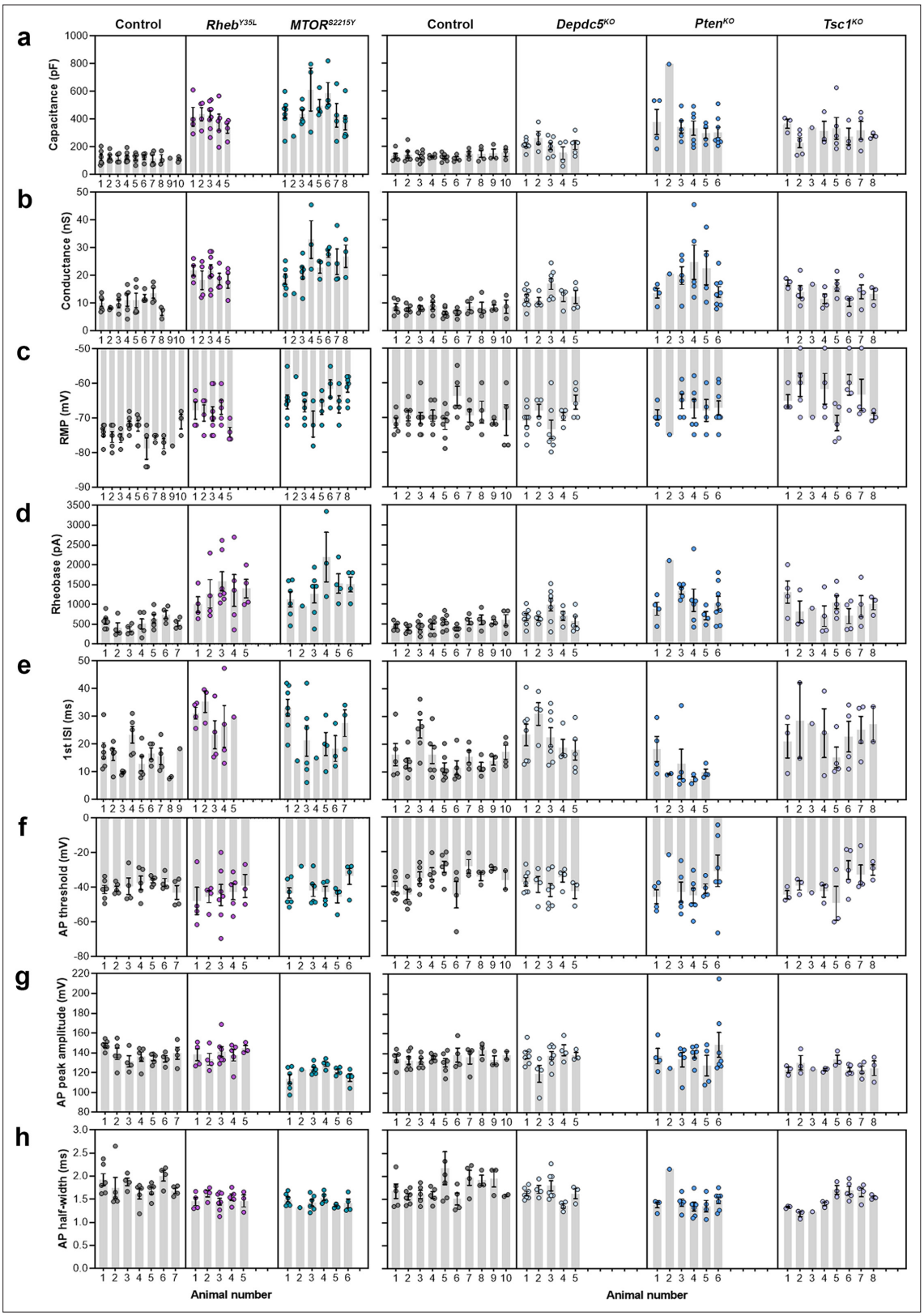

Figure 2—figure supplement 1. Distribution of membrane and action potential (AP) properties among individual animals at P26-51. (**a–c**) Distribution of membrane capacitance, conductance, and resting membrane potential (RMP) among individual animals. (**d-h**) Distribution of rheobase, first ISI, AP threshold, AP peak amplitude, and AP half-width among individual animals.

Figure 3. Expression of *Rheb*^{Y35L}, *MTOR*^{S2215Y}, *Depdc5*^{KO}, *Pten*^{KO}, and *Tsc1*^{KO} leads to the abnormal presence of HCN4 channels with variations in functional expression. (**a**) Representative images of tdTomato+ cells (red) and HCN4 staining (green) in mouse medial prefrontal cortex (mPFC) at P28-43. (**b**) Quantification of HCN4 intensity (normalized to the mean control) in tdTomato+ neurons. (**c**) Representative current traces in response to a series of 3 s-long hyperpolarizing voltage steps from –120 to –40 mV, with a holding potential of –70 mV. Current traces from the –40 and –50 mV steps were not included due to contamination from unclamped Na^+ spikes. Orange lines denote the current traces at –90 mV. (**d**) IV curve obtained from I_{ss} amplitudes. (**e**) ΔIV curve obtained from I_h amplitudes (i.e. ΔI, where $\Delta I = I_{ss} - I_{inst}$). (**f**) Graphs of I_h amplitudes at –90 mV. (**g**) Representative current traces in response to a series of 3 s long hyperpolarizing voltage steps from –110 mV to –50 mV in the *MTOR*^{S2215Y} condition pre- and post-zatebradine

Figure 3 continued on next page

Figure 3 continued

application. Orange lines denote the current traces at –90 mV. (**h**) IV curve obtained from I_{ss} amplitudes in the *MTOR*^{S2215Y} condition pre- and post-zatebradine application. (**i**) ΔIV curve obtained from I_h amplitudes (i.e. ΔI) in the *MTOR*^{S2215Y} condition pre- and post-zatebradine application. Arrow points to the post-zatebradine I_h amplitude at –90 mV. (**j**) Representative traces of the zatebradine-sensitive current obtained after subtraction of the post- from the pre-zatebradine current traces in response to –110 mV to –50 mV voltage steps. Orange lines denote the current traces at –90 mV. (**k**) IV curve of the zatebradine-sensitive current obtained after subtraction of the post- from the pre-zatebradine current traces. (**l**) Graph of RMP in the control and *MTOR*^{S2215Y} conditions pre- and post-zatebradine application. Connecting lines denote paired values from the same neuron. For graph (**b**): n=4–8 mice per group, with 4–15 cells analyzed per animal. For graphs **d, e, f**: n=5–10 mice per group, with 24–47 cells analyzed per animal. For graphs **h, i, k, l**: n=4–6 neurons (paired). Statistical comparisons were performed using (**b, f**) nested ANOVA (fitted to a mixed-effects model) to account for correlated data within individual animals, (**d, e**) mixed-effects ANOVA accounting for repeated measures, or (**h, i, l**) two-way repeated measures ANOVA. Post-hoc analyses were performed using Holm-Šídák multiple comparison test. *p<0.05, **p<0.01, ****p<0.0001, for the IV curves in **d, e, h, i**: *p<0.05 (vs. control), #p<0.05 (vs. *Rheb*^{Y35L} or *Depdc5*^{KO}), ϒp<0.05 (vs. *Pten*^{KO}). All data are reported as the mean of all neurons in each group ± SEM.

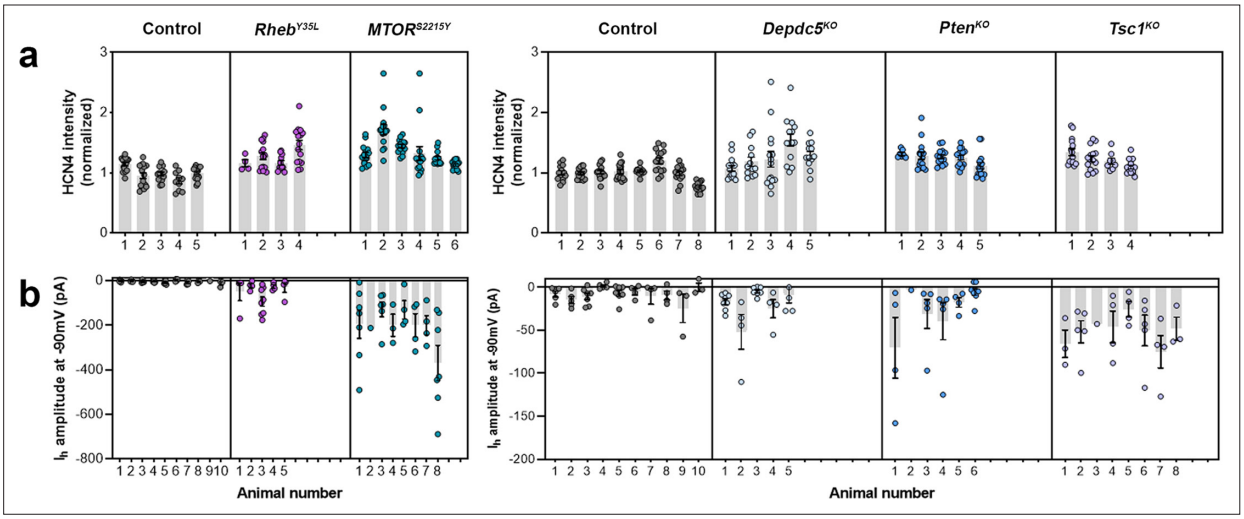

Figure 3—figure supplement 1. Distribution of HCN4 staining intensity and hyperpolarization-activated cation current (I_h) amplitudes (at –90 mV) among individual animals at P28-43 and P26-51, respectively. (**a**) Distribution of HCN4 staining intensity among individual animals. (**d-g**) Distribution of I_h amplitudes (at –90 mV) among individual animals.

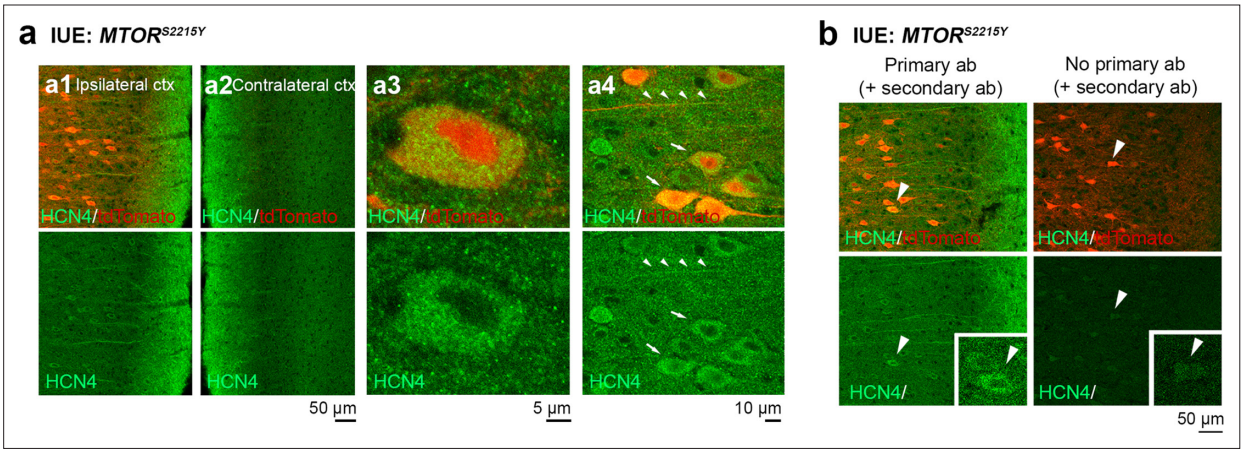

Figure 3—figure supplement 2. Additional images of HCN4 staining in medial prefrontal cortex (mPFC) sections from P28-43 mice expressing *MTOR*^{S2215Y}. (**a**) Representative images of tdTomato+ cells (red) and HCN4 staining (green). Top panels show overlay images. Bottom panels show HCN4 single-channel images. (**a1**) and (**a2**) show the ipsilateral and contralateral cortex, respectively. (**a3**) and (**a4**) are high-magnification images demonstrating HCN4 staining within the cell. (**b**) Representative images of immunostaining with (left) or without (right) HCN4 primary antibodies (control for secondary antibody specificity).

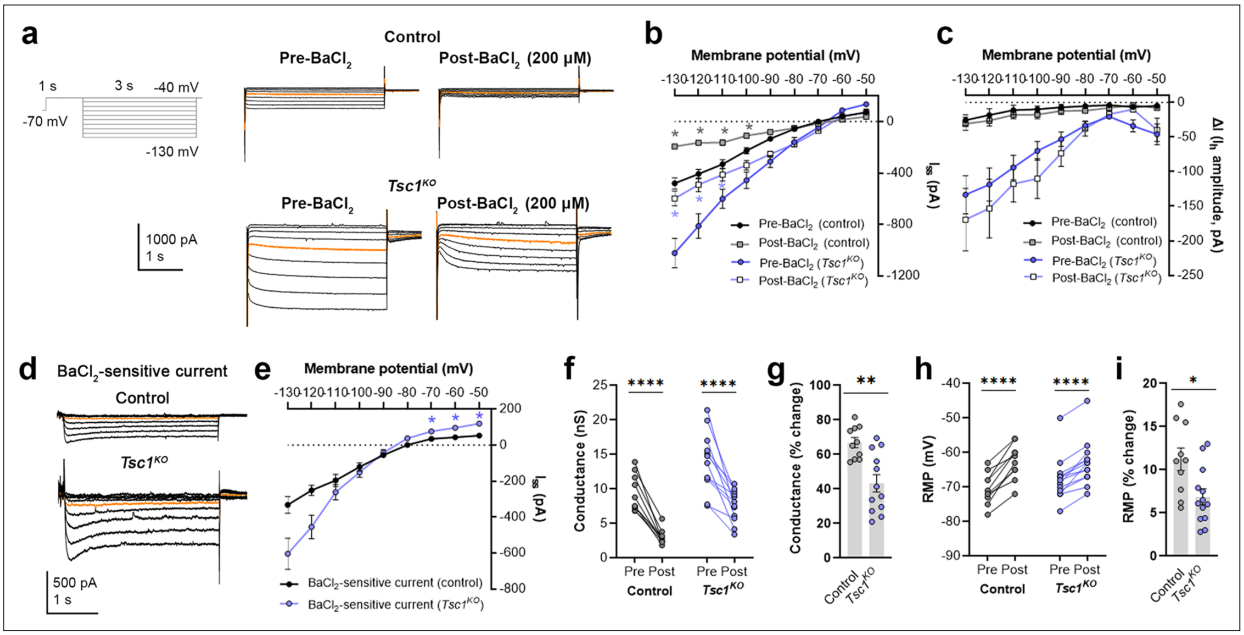

Figure 3—figure supplement 3. $BaCl_2$ application decreases overall inward currents without affecting hyperpolarization-activated cation current (I_h) in *Tsc1*^{KO} neurons. (**a**) Representative current traces in response to a series of 3 s long hyperpolarizing voltage steps from –130 mV to –40 mV in the *Tsc1*^{KO} condition pre- and post-$BaCl_2$ application. Orange lines denote the current traces at –90 mV. (**b**) IV curve obtained from I_{ss} amplitudes in the *Tsc1*^{KO} condition pre- and post-$BaCl_2$ application. (**c**) IV curve obtained from I_h amplitudes (i.e. ΔI, where $\Delta I = I_{ss} - I_{inst}$) in the *Tsc1*^{KO} condition pre- and post-$BaCl_2$ application. (**d**) Representative traces of the $BaCl_2$-sensitive current obtained after subtraction of the post- from the pre-$BaCl_2$ current traces. Orange lines denote the current traces at –90 mV. (**e**) IV curve of the $BaCl_2$ -sensitive current obtained after subtraction of the post- from the pre-$BaCl_2$ current traces. The isolated $BaCl_2$-sensitive current reversed near –80 mV. (**f**) Graph of conductances (at –500 pA) in the control and *Tsc1*^{KO} conditions pre- and post-$BaCl_2$ application. Connecting lines denote paired values from the same neuron. (**g**) Graph of % change in conductances pre- and post-$BaCl_2$ application in the control and *Tsc1*^{KO} conditions. (**h**) Graph of resting membrane potential (RMP) in the control and *Tsc1*^{KO} conditions pre- and post-$BaCl_2$ application. Connecting lines denote paired values from the same neuron. (**i**) Graph of % change in RMP pre- and post-$BaCl_2$ application in the control and *Tsc1*^{KO} conditions. For all graphs: n=10–13 neurons per group. Statistical comparisons were performed using (**b, c, e**) mixed-effects ANOVA, (**f, h**) two-way repeated measures ANOVA, or (**g, i**) unpaired t-test. Post-hoc analyses were performed using Holm-Šídák multiple comparison test. *p<0.05, **p<0.01, ****p<0.0001. All data are reported as the mean of all neurons or brain sections in each group ± SEM.

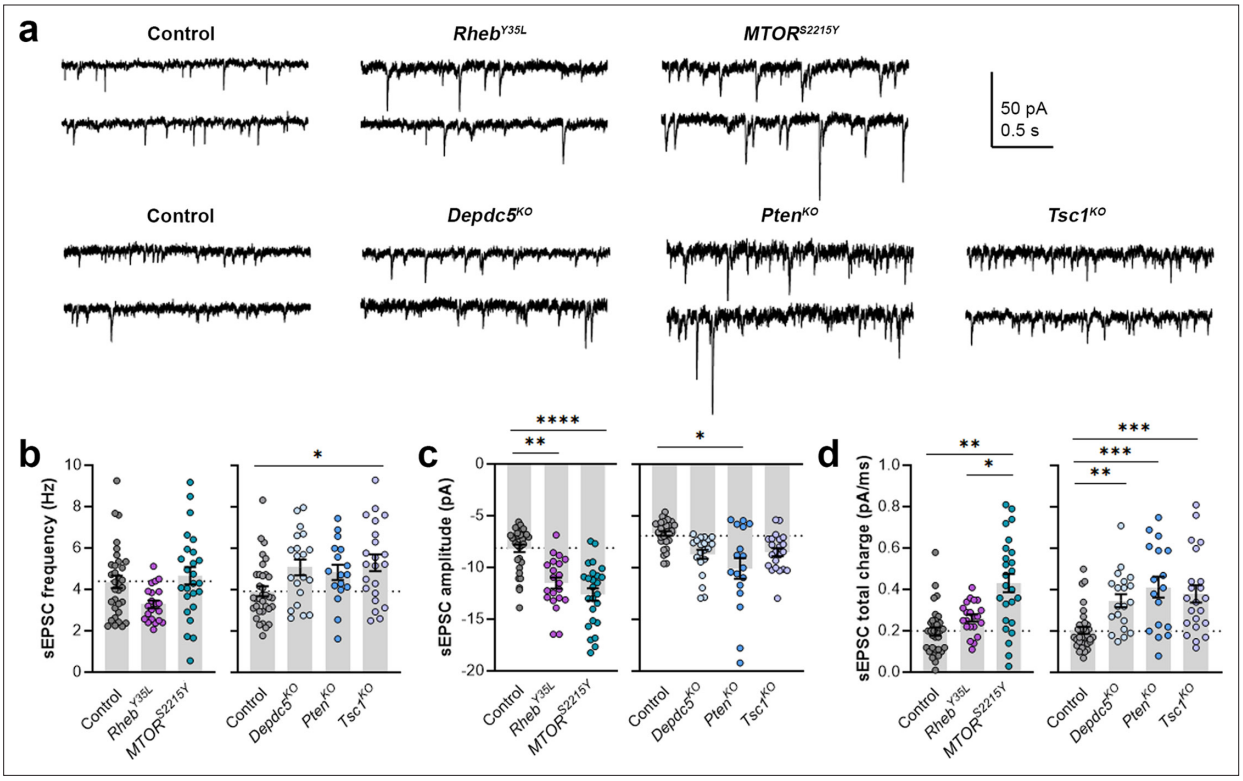

Figure 4. Expression of *Rheb*^{Y35L}, *MTOR*^{S2215Y}, *Depdc5*^{KO}, *Pten*^{KO}, and *Tsc1*^{KO} leads to different impacts on spontaneous excitatory postsynaptic current (sEPSC) properties. (**a**) Representative sEPSC traces were recorded at a holding voltage of –70 mV. Top and bottom traces are from the same neuron. (**b–d**) Graphs of sEPSC frequency, amplitude, and total charge. For all graphs: n=5–9 mice per group, with 17–34 cells analyzed per animal. Statistical comparisons were performed using a nested ANOVA (fitted to a mixed effects model) to account for correlated data within individual animals. Post-hoc analyses were performed using Holm-Šídák multiple comparison test. *p<0.05, **p<0.01, ***p<0.001, ****p<0.0001. All data are reported as the mean of all neurons in each group ± SEM.

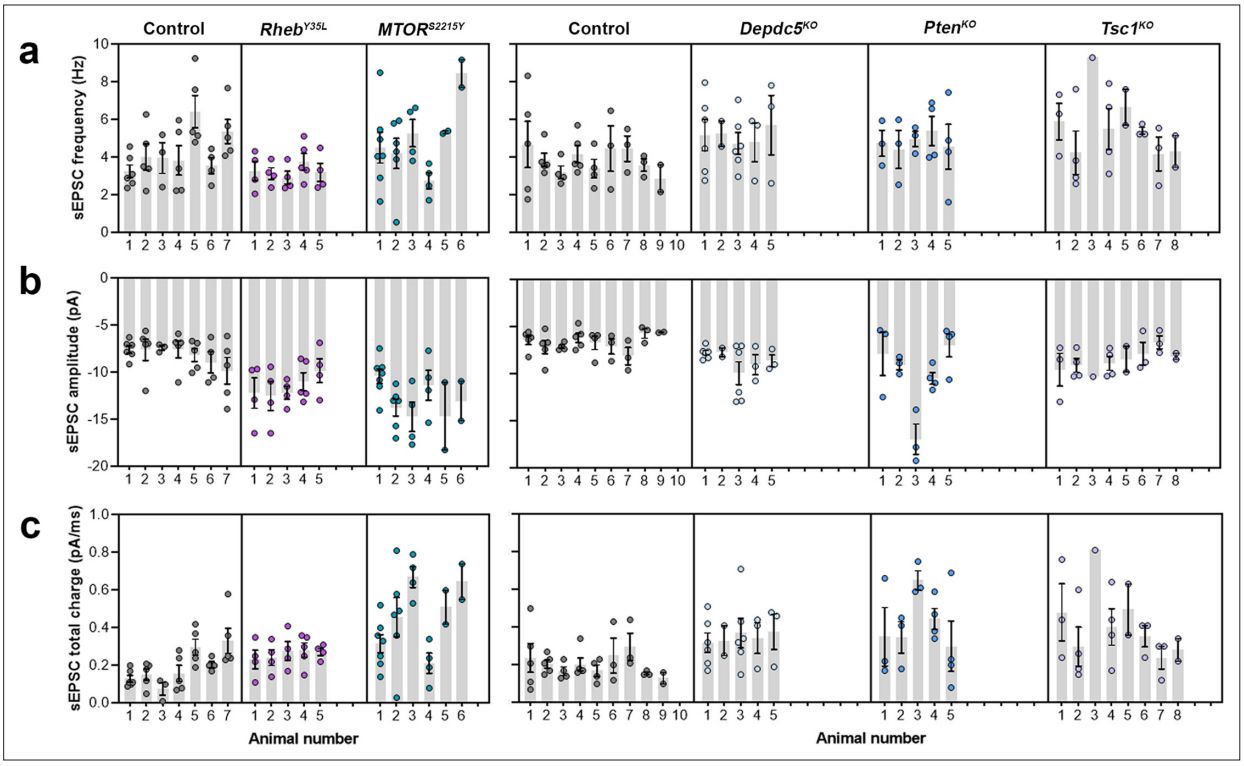

Figure 4—figure supplement 1. Distribution of spontaneous excitatory postsynaptic current (sEPSC) properties among individual animals at P26-51. (**a–c**) Distribution of sEPSC properties among individual animals.